

Dark and visible matter in spiral galaxies

M. Persic^{★, 1, 2} and P. Salucci^{3, 4}

¹Laboratory for High Energy Astrophysics, NASA Goddard Space Flight Center, Greenbelt, MD 20771, USA

²Osservatorio Astronomico, via G. B. Tiepolo 11, I-34131 Trieste, Italy

³SISSA, Strada Costiera 11, I-34014 Trieste, Italy

⁴Physics Department, Durham University, Durham DH1 3LE

Accepted 1988 February 19. Received 1988 February 19; in original form 1987 March 25

Summary. Exploiting relevant information from the profiles of rotation curves, we calculate the dark-to-luminous mass ratio within the disc size for a sample of 43 spiral galaxies. The values we find, while proving the ubiquitous presence of dark matter, vary with luminosity. Faint and bright galaxies are found to be respectively halo- and disc-dominated in the disc regions. The luminosity sequence turns out to be a dark-to-luminous sequence.

The Tully–Fisher correlation is justified as connected with the equilibrium condition of a thin disc embedded in a spherical halo. The dynamical effect of dark matter does not disrupt such a centrifugal equilibrium, because the dark-matter mass fraction is a smooth function of luminosity. By removing the dark-matter contribution from the velocity at the disc edge, the dispersion affecting the luminosity–kinematics relation is dramatically decreased as compared with the conventional Tully–Fisher correlation ($\Delta\sigma \approx 0.3$ mag).

Comparison with stellar evolution models shows that the dynamically computed $(M/L_B)_{\text{disc}}$ ratios are able to explain the colours of spiral galaxies in a scenario involving a 10-Gyr star-formation phase with $H_0 = 75 \text{ km s}^{-1} \text{ Mpc}^{-1}$.

1 Introduction

The fairly flat shapes of the rotation curves of spiral galaxies provide strong evidence for the presence of (possibly large) amounts of dark matter even within the limits of the optical disc (Rubin *et al.* 1980, 1982, 1985; Carignan & Freeman 1985). However, the decomposition of matter distribution into a visible and a dark component based on dynamical considerations is

[★]NRC/NAS Resident Research Associate.

highly uncertain and controversial (Burstein & Rubin 1985; Carignan & Freeman 1985; Bahcall & Casertano 1985; van Albada *et al.* 1985; Kent 1986; van Albada & Sancisi 1986). In fact, the evaluation of integral properties (such as the amount of dark matter within the optical size) depends quite sensitively on the assumptions on mass distribution, so that a systematic, self-consistent study of the halo and disc properties has not been proposed so far.

In addition, difficulties in studying the present properties of galaxies arise from the lack of theoretical knowledge of the late stages of galaxy formation. The assumed cosmological scenario, the physics of disc formation and the present structure of spirals are so tightly interwoven that they seem to elude separate investigations.

One more puzzle is the featureless appearance of rotation curves. These look rather similar to each other. Their shapes, in fact, do not appear to show any evidence for either different mass components within each galaxy or for the galaxies' individual integral characteristics. This lack of information occurs in spite of the large ranges spanned by the galaxies' scale properties. Moreover, since within the optical disc luminous matter contributes sensitively to the dynamics ($\langle M_{\text{lum}} \rangle \sim 1/2 \langle M_{\text{dyn}} \rangle$, Rubin *et al.* 1985), we require that the dark and the luminous mass distributions finely combine in order to produce a smooth rotation curve. Such a smoothness is likely to be the output of some dynamical processes which caused a fine tuning in the disc-halo structure parameters, washing away any feature which possibly marked the boundary between disc-dominated and halo-dominated regions (e.g. Blumenthal *et al.* 1986). In view of these issues it becomes then a question of whether we can actually obtain some fundamental galaxy properties, such as the luminous-to-dark mass ratio and the halo mass, from others which are directly observable.

The aim of this paper is to derive such fundamental galaxy properties by using a method which almost exclusively relies on the observed properties of luminous (i.e. photometry) and total (i.e. rotation curves) matter and minimizes the importance of the assumptions we shall make on dark matter.

A decisive step in this direction is the straight exploitation of the whole information stored in the axisymmetric circular velocity fields of spirals. This strategy is suggested by the results of our previous paper (Persic & Salucci 1986, henceforth Paper I), where it is shown that by using both the maximum velocity and its mean gradient (i.e. the amount of the total matter and its radial distribution), one can build up an excellent indicator of galactic luminosities and sizes which proves to be a more reliable one than the mere maximum velocity.

The plan of this paper is as follows. After discussing the photometric properties and rotation curves of galaxies (Section 2) and arguing for the existence of dark matter in virtually spherical haloes from the profiles of the central-velocity fields (Section 3), we investigate the systematics of dark matter (i.e. the dark-to-luminous mass ratios within the optical sizes) from the systematics of

Table 1. Observational properties of galaxies (see text for their definitions) and references for kinematics and photometry. Lengths are in kpc, velocities in km s^{-1} . Colours are taken from RC2 or from Whitmore (1984). Due to lack of published data, a few galaxies have been assigned colours typical for their respective Hubble types, following de Vaucouleurs and de Vaucouleurs (1972).

Galaxy	M_B	R_I	$R_{2.5}$	$V_{2.5}$	\bar{V}	R_D	$(B-V)_0$	Type	P	K
N 2998	-22.79	7.0	40.0	228.6	52.4	8.3	0.54	Sc	9	1
N 4605	-18.59	1.5	4.4	118.8	8.3	1.0	...	Sc	9	1
N 801	-23.31	9.0	53.8	202.8	67.9	13.0	0.54	Sc	9	1
N 3495	-21.31	4.0	15.5	197.2	22.3	4.9	0.54	Sc	9	1
N 1421	-22.15	7.0	19.6	205.3	28.3	8.3	0.25	Sc	9	1

Table 1 – continued

Galaxy	M_B	R_I	$R_{2.5}$	$V_{2.5}$	\bar{V}	R_D	$(B-V)_0$	Type	P	K
N 2608	-20.74	4.0	15.2	148.9	19.0	3.0	0.40	Sc	9	1
N 2742	-20.54	3.0	12.6	192.1	31.5	3.8	0.46	Sc	9	1
N 4062	-19.50	0.5	9.0	167.3	26.0	4.1	0.62	Sc	9	1
N 1035	-19.69	2.0	7.6	139.6	21.9	2.3	0.64	Sc	9	1
IC 467	-21.35	6.0	21.5	154.9	31.8	4.7	0.54	Sc	9	1
N 1087	-21.30	4.0	15.6	157.0	25.3	4.6	0.46	Sc	9	1
N 3054	-21.63	5.0	25.7	264.2	51.8	5.4	0.42	Sb	9	2
N 7537	-21.23	4.0	18.3	137.3	40.4	3.7	0.42	Sb	9	2
N 2815	-22.00	6.0	26.5	283.5	74.6	9.2	0.74	Sb	9	2
N 7606	-22.54	10.0	39.8	242.0	87.7	8.3	0.59	Sb	9	2
N 3200	-22.87	10.0	46.0	287.7	71.8	14.8	0.60	Sb	9	2
U12810	-23.06	16.0	51.8	234.0	58.1	11.2	0.74	Sb	9	2
N 1620	-22.06	4.0	29.8	279.6	43.9	8.9	0.60	Sb	9	2
N 1085	-22.88	8.0	34.8	310.0	89.3	10.0	0.74	Sb	9	2
N 1325	-20.87	4.0	18.8	211.7	30.4	5.7	0.59	Sb	9	2
N 2708	-20.60	4.0	14.7	293.3	36.2	4.3	0.74	Sb	9	2
N 1417	-22.28	1.5	33.7	328.6	67.4	8.0	0.74	Sb	9	2
N 3067	-20.33	3.0	9.6	162.2	30.0	3.3	0.54	Sb	9	2
N 5290	-21.61	10.2	26.4	230.0	57.1	5.5	0.54	Sb	2	6
N 4682	-20.85	5.0	17.5	183.9	38.9	4.8	0.54	Sc	9	1
N 7541	-22.30	6.0	28.5	278.0	39.8	9.7	0.60	Sbc	9	1
N 4321	-21.53	5.0	20.1	222.4	50.1	6.9	0.69	Sc	5	1
N 2715	-21.21	3.0	20.4	158.2	30.3	8.9	0.49	Sc	5	1
N 7171	-21.25	5.0	23.9	226.8	56.3	7.4	0.66	Sb	9	2
N 5383	-22.50	8.0	22.0	207.0	65.7	6.0	0.64	Sb	4	8
N 7331	-22.40	12.0	34.1	226.0	57.7	10.6	0.68	Sbc	3	12
N 5033	-21.30	10.0	28.0	211.5	54.3	12.0	0.71	Sc	5	12
N 2336	-22.50	13.3	46.2	251.0	71.4	15.8	0.58	Sbc	3	5
N 5905	-22.32	16.2	41.3	242.0	61.6	16.4	0.54	Sb	2	4
N 4254	-21.51	1.9	15.6	210.0	41.6	4.4	0.55	Sc	5	13
N 3963	-22.37	9.9	27.8	177.5	50.2	7.4	0.62	Sbc	6	14
N 4565	-23.00	7.0	46.6	254.0	74.4	13.2	0.68	Sb	7	12
N 3992	-21.70	9.7	24.6	273.0	60.0	8.8	0.77	Sbc	4	11
N 5426	-21.24	5.0	20.3	157.0	46.1	6.3	0.52	Sc	1	7
N 3898	-20.50	1.0	14.7	252.0	50.0	7.0	0.83	Sab	3	3
N 488	-22.52	2.0	36.0	385.0	91.0	10.4	0.83	Sb	3	9
N 2639	-21.90	5.0	19.2	350.0	85.4	3.2	0.84	Sa	8	3
N 3504	-20.75	3.0	11.5	187.0	31.7	4.8	0.63	Sab	2	10

References:

Photometry (P): (1) Blackman 1982; (2) Blackman & van Moorsel 1984; (3) Boroson 1981; (4) Elmegreen & Elmegreen 1984; (5) Elmegreen & Elmegreen 1985; (6) Grosbol 1985; (7) Hamabe 1982; (8) Kent 1984; (9) Kent 1986.

Kinematics (K): (1) Rubin *et al.* 1980; (2) Rubin *et al.* 1982; (3) Rubin *et al.* 1985; (4) van Moorsel 1982; (5) van Moorsel 1983b; (6) van Moorsel 1983c; (7) Blackman 1982; (8) Sancisi *et al.* 1979; (9) Peterson 1980; (10) Peterson 1982; (11) Gottesman *et al.* 1984; (12) Bosma 1981; (13) Chincarini & de Souza 1985; (14) van Moorsel 1983a.

rotation curves (i.e. their mean gradients) in Section 4. We then discuss the derived disc properties and provide a theoretical justification for the Tully–Fisher correlation. In particular, we consider how systematic variations of the dark-mass fraction along the luminosity sequence affect the Tully–Fisher correlation. We also compare the derived disc mass-to-light ratios with those predicted by stellar-evolution models (Section 5). The results are discussed in the context of different dark versus visible mass decomposition methods in Section 6 and summarized in Section 7.

The sample of galaxies (henceforth sample C, samples A and B are studied in Paper I) to which we apply our structure-solving method comprises all (43) non-local Sa–Sc galaxies for which both photometry and high-quality extended rotation curves are available in the literature. The observational data for these galaxies are listed in Table 1. Local galaxies are left out in order to avoid the admixture of galaxies whose distances are obtained from local calibrators with galaxies whose distances are determined from redshifts. Throughout the paper we use $H_0=50 \text{ km s}^{-1} \text{ Mpc}^{-1}$.

2 Spiral galaxies: photometry, rotation curves and dark matter

In this section we address the spirals’ observed properties which are the starting point to any structure model. Since a discrepancy between the luminous mass and the dynamically inferred mass is a piece of evidence common to virtually all spiral galaxies, we shall ignore occasional and peculiar features (e.g. strong bars, warps, non-exponential discs, bulge-dominated systems), which in any case affect a very small fraction, if any, of our sample galaxies.

2.1 DISTRIBUTION OF LIGHT

The luminosity profiles of most galaxies are decomposed into two main components (Freeman 1970; Boroson 1981; Simien & de Vaucouleurs 1986; van der Kruit 1987). These are, respectively, a very concentrated bulge and a thin disc, whose surface luminosity density decreases with radius as

$$I(R)=I_0 \exp(-R/R_D), \quad (1)$$

I_0 being the central surface luminosity density and R_D the exponential disc length-scale.

The bulge is usually less luminous and smaller than the disc. Typically, their relative luminosities and sizes are: $L_B/L_D=0.7-0.1$ and $R_{25}/R_B=8-16$ for Sa–Sc galaxies (Simien & de Vaucouleurs 1986) (R_B is the effective bulge radius). Thus, for a typical value of $(\mathcal{M}/L)_{\text{bulge}}\sim 7$ (as for ellipticals), the bulge contribution to the equilibrium structure is usually negligible at radii $R\geq 2R_B$. This turns out to be actually the case, as the outer profiles of rotation curves are not correlated with the bulge-to-disc light ratio (Rubin *et al.* 1985). From equation (1) the surface brightness at radius R is

$$\mu(R)=\mu_0+1.1 R/R_D, \quad (2)$$

with μ_0 having a small scatter among spirals (Freeman 1970; van der Kruit 1987):

$$\mu_0=21.7\pm 0.4 \text{ mag arcsec}^{-2}, \quad (3)$$

which implies

$$R_{25}/R_D=3.0\pm 0.4 \quad (4)$$

where R_{25} is the 25 B -mag arcsec^{-2} contour. The values of the disc length-scales R_D for sample C were obtained from available photometry and are shown in Table 1. r photometry has been transformed into B photometry by means of the transformation: $B-r=1$. The luminosity profiles

of galaxies not found already decomposed into bulge and disc components have been successfully fitted in their outer parts ($R > 0.5 R_{25}$) with the exponential thin-disc model (2) in order to obtain their disc length-scales.

As a general property, colours show no substantial gradient across discs (Griersmith 1980). This strongly suggests a *constant stellar mass-to-light ratio* in each galaxy. Then we can write

$$R \left(\frac{d\phi}{dR} \right)_{\text{lum}} \simeq R \left(\frac{d\phi}{dR} \right)_{\text{disc}} = V_{\text{disc}}^2(R) \quad (5)$$

where ϕ_{lum} is the gravitational potential due to all luminous matter and $V_{\text{disc}}(R)$ is the circular velocity of the exponential thin-disc model (Freeman 1970),

$$V_{\text{disc}}^2(R) = G \mathcal{M}_D / R_D F(x) \quad (6)$$

where \mathcal{M}_D is the disc mass, $x = R/R_D$ and $F(x) = 1/2 x^2 (I_0 K_0 - I_1 K_1)$ with I_n and K_n the modified Bessel functions of order n evaluated at $x/2$.

2.2 ROTATION CURVES

As a very general property, virtually all extended optical rotation curves show a *constant gradient* in the region $R_1 = (0.1-0.2) R_{25} \leq R \leq R_{25}$. By fitting the observed rotation velocity $V_{\text{obs}}(R)$ in this region with the simple linear function

$$V(R) = V_0 + V_1 R / R_{25}, \quad (7)$$

we found that for all galaxies of sample C, equation (7) fits the observed circular velocity to a high level of confidence (see also Persic & Salucci 1985, Salucci 1986; Paper I). Moreover, the residuals $\Delta V(R) = V_{\text{obs}}(R) - V(R)$ show no large-scale features, proving their non-axisymmetric local origin (mainly due to the spiral gravitational potential) (Salucci 1986). Therefore, in the range $R_1 < R < R_{25}$ we can assume a simple straight line to represent the circular velocity, in implicit agreement with similar results in the literature (e.g. Rubin *et al.* 1980). Thus, we obtain the maximum of the circular velocity $V_M = \text{MAX} \{V_0 + V_1, V_0 + V_1 R_1 / R_{25}\}$ and its gradient V_1 / R_{25} by using the overall shape of the rotation curve. The internal fractional errors are 5 per cent in V_{25} and 5–20 per cent in V_1 (Paper I). The coefficients of the fits, V_0 and V_1 , for the galaxies of sample C are reported in Salucci (1986) and in Table 1 by means of the combinations $V_{25} = V_0 + V_1$ and $\bar{V} = V_{25} [1 - 1/\sqrt{2(1 + V_1/V_{25})}]^{1/2}$.

We note that in a few cases an extrapolation of the circular velocity from the last measured point to R_{25} was required in order to study the properties of some faint galaxies at the same isophotal radius as the other galaxies of the sample.

2.3 DARK MATTER: THE MASS-TO-LIGHT RATIO

The (dynamical mass)-to-light ratio is a distance-dependent quantity. In addition, the amount of luminous mass cannot be inferred straightforwardly from the observed luminosity. In spite of these concerns, however, when a large sample of galaxies is examined and different samples are compared, an important though qualitative picture emerges. Let us define the light-to-mass ratio as

$$L / \mathcal{M}_{\text{dyn}} = GL / (V_{25}^2 R_{25}) \quad (8)$$

where L is the luminosity in a given waveband, and the luminous-to-total mass ratio as

$$\mathcal{M}_{\text{lum}} / \mathcal{M}_{\text{dyn}} \equiv L / \mathcal{M}_{\text{dyn}} (\mathcal{M} / L)_* \quad (9)$$

where $(\mathcal{M} / L)_*$ is the stellar mass-to-light ratio in the same band.

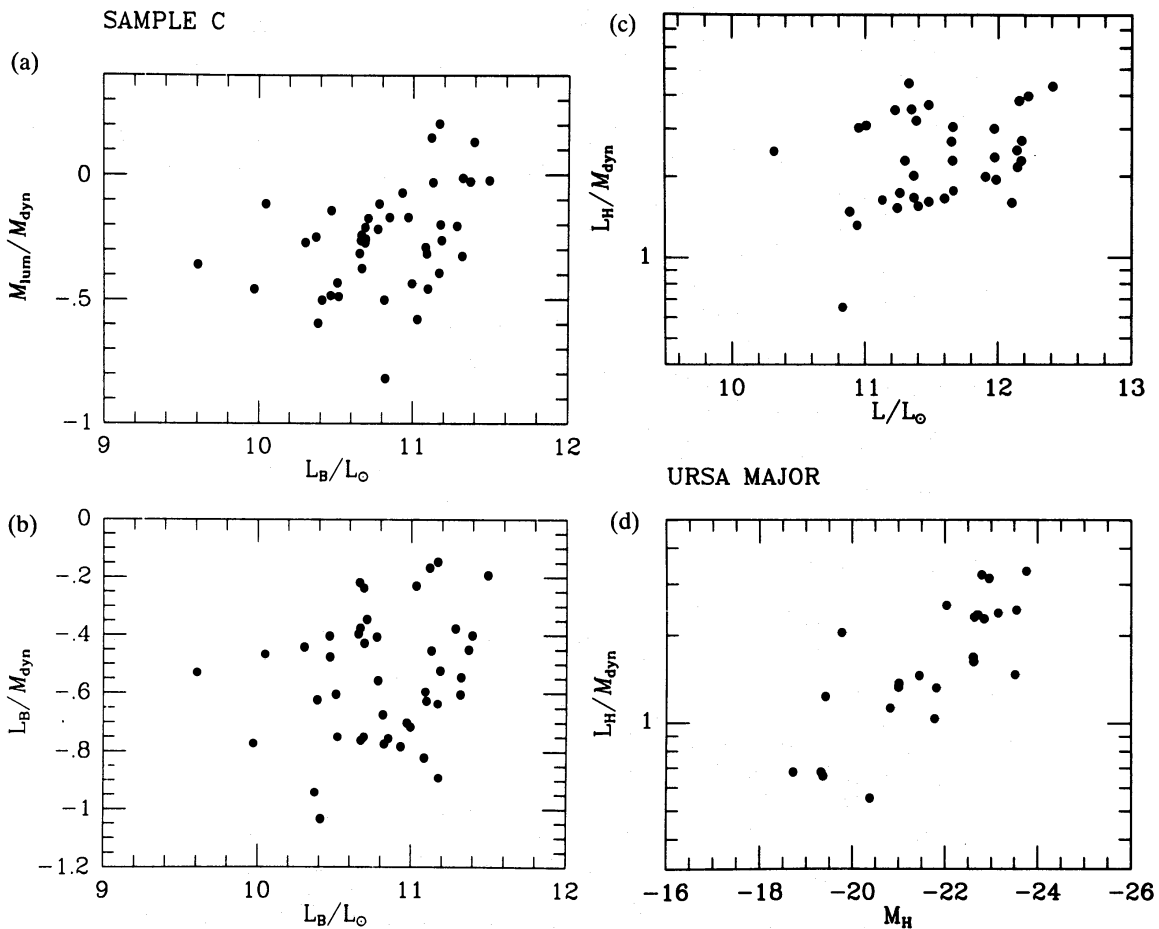


Figure 1. (a) Luminous-to-dynamical mass ratios for sample C. The Larson–Tinsley stellar-evolution model has been used to obtain stellar mass-to-light ratios from galaxy colours (ratios and luminosities are in decimal logarithm). (b) Light-to-mass ratios in the blue band for sample C. (c) Light-to-mass ratios in the infrared band for sample C. (d) Light-to-mass ratios in the infrared band for a sample in the Ursa Major cluster.

In Fig. 1(a)–(d) we plot these visible-to-total mass indicators versus galaxy luminosities for sample C in both the blue and infrared wavebands and for a sample containing galaxies in the Ursa Major cluster with available IR magnitudes and 21-cm linewidths (Aaronson *et al.* 1982).

We have considered the IR band because it is likely to better reflect the underlying disc population. Moreover, we investigated an additional sample within a cluster in order to check the obtained results in a sample free from problems connected with the determination of galactic distances.

We find the following results (see Fig. 1):

(i) Visible matter gives an important contribution to the galaxies’ structures in the regions within the optical discs. We can therefore rule out degenerate solutions where virtually all the mass resides in the dark component, and set up the (averaged) limits

$$\begin{aligned} \langle \mathcal{M}_{dark}/\mathcal{M}_{vis} \rangle &< 5 (H_0/50) \langle (\mathcal{M}/L)_{LT} \rangle / \langle (\mathcal{M}/L)_* \rangle, & M_B \sim -19 \\ \langle \mathcal{M}_{dark}/\mathcal{M}_{vis} \rangle &< 0.5 (H_0/50) \langle (\mathcal{M}/L)_{LT} \rangle / \langle (\mathcal{M}/L)_* \rangle, & M_B \sim -22 \end{aligned} \quad (10)$$

where $(\mathcal{M}/L)_{LT}$ is the stellar mass-to-light ratio following the Larson–Tinsley evolutionary

model (Tinsley 1981, henceforth LT). It is important to realize that for each galaxy there is a minimum disc mass $\sim 1/2 L_{\text{disc}}(\mathcal{M}/L)_{\text{LT}}$ which is compatible with the LT model and with the maximum realistic error which may possibly affect the determination of distances.

(ii) There is a markedly positive trend between luminosity and dynamical importance of dark matter. Faint galaxies tend to be dark-matter dominated, and the brighter is the galaxy the lesser is the relative dark-matter contribution to the structure. Looking at *integral* mass indicators, very bright galaxies do not definitely show the presence of dark matter within the optical size.

Such results on the dark-to-visible mass coupling disagree with the view of van Albada *et al.* (1985), where it is claimed that galactic structures are largely undetermined due to poor knowledge of the dark-matter dynamical properties. As a matter of fact, if we assume an equilibrium solution with given values \mathcal{M}_{H} and \mathcal{M}_{D} for the dark-halo and disc masses inside R_{25} (e.g. the solution corresponding to the maximum-disc hypothesis) respectively, we cannot indefinitely build up new solutions with progressively less matter in the disc and more mass in the halo unless we violate the constraint imposed by equation (10). In other words, observed colours and stellar-evolution models rule out the case of a negligibly small disc mass.

In the following section we shall therefore investigate how narrow are the ranges spanned by the galaxies' basic properties and structure models allowed by the constraints discussed above.

3 Where is dark matter?

In order to understand at what radius in each galaxy the discrepancy between visible and dynamical mass begins, we need a local mass indicator which avoids the problem of translating disc luminosity into disc mass. To this purpose let us define the quantities $a_{\text{D}}(R)$ and $a(R)$ respectively as

$$a_{\text{D}}(R) \equiv \frac{\tilde{V}_{\text{disc}}(R)}{V_{\text{disc}}(R)} = 1 - \left[0.5 + \frac{I_0 K_0 + 0.5x(I_1 K_0 - I_0 K_1)}{2(I_0 K_0 - I_1 K_1)} \right]^{1/2} \quad (11a)$$

and

$$a(R) \equiv \tilde{V}(R)/V(R), \quad (11b)$$

where

$$\tilde{V}_{\text{disc}}(R) \equiv V_{\text{disc}}(R) \{1 - 1/\sqrt{2} [1 + d \log V_{\text{disc}}(R)/d \log R]^{1/2}\} \quad (12a)$$

and

$$\tilde{V}(R) \equiv V(R) \{1 - 1/\sqrt{2} [1 + d \log V(R)/d \log R]^{1/2}\}. \quad (12b)$$

Our aim is then to compare the logarithmic gradients of the circular velocities predicted by the exponential thin-disc model with the observed ones. While many functions of the logarithmic gradient would be suitable to this purpose, we have chosen equation (11) in order to more easily link the results on galaxy structure obtained in this paper with the phenomenological ones found in Paper I.

In Fig. 2 we plot the quantities a_{D} and a versus radius for each galaxy of the sample. Obviously, if the disc matter were the only component contributing to the dynamics, we would find $a_{\text{D}} \approx a$ over the whole disc. In each and every galaxy we find, on the contrary, a dramatic discrepancy between these two quantities. In regions where $a_{\text{D}} > a$ this discrepancy cannot be eliminated nor even reduced by introducing possible contributions from a bulge and/or a stellar halo. In fact, the stellar halo has a very steep radial density profile (Bahcall *et al.* 1983) and the bulge is seen as a point-mass from the outermost disc regions. Then, it is easy to realize that

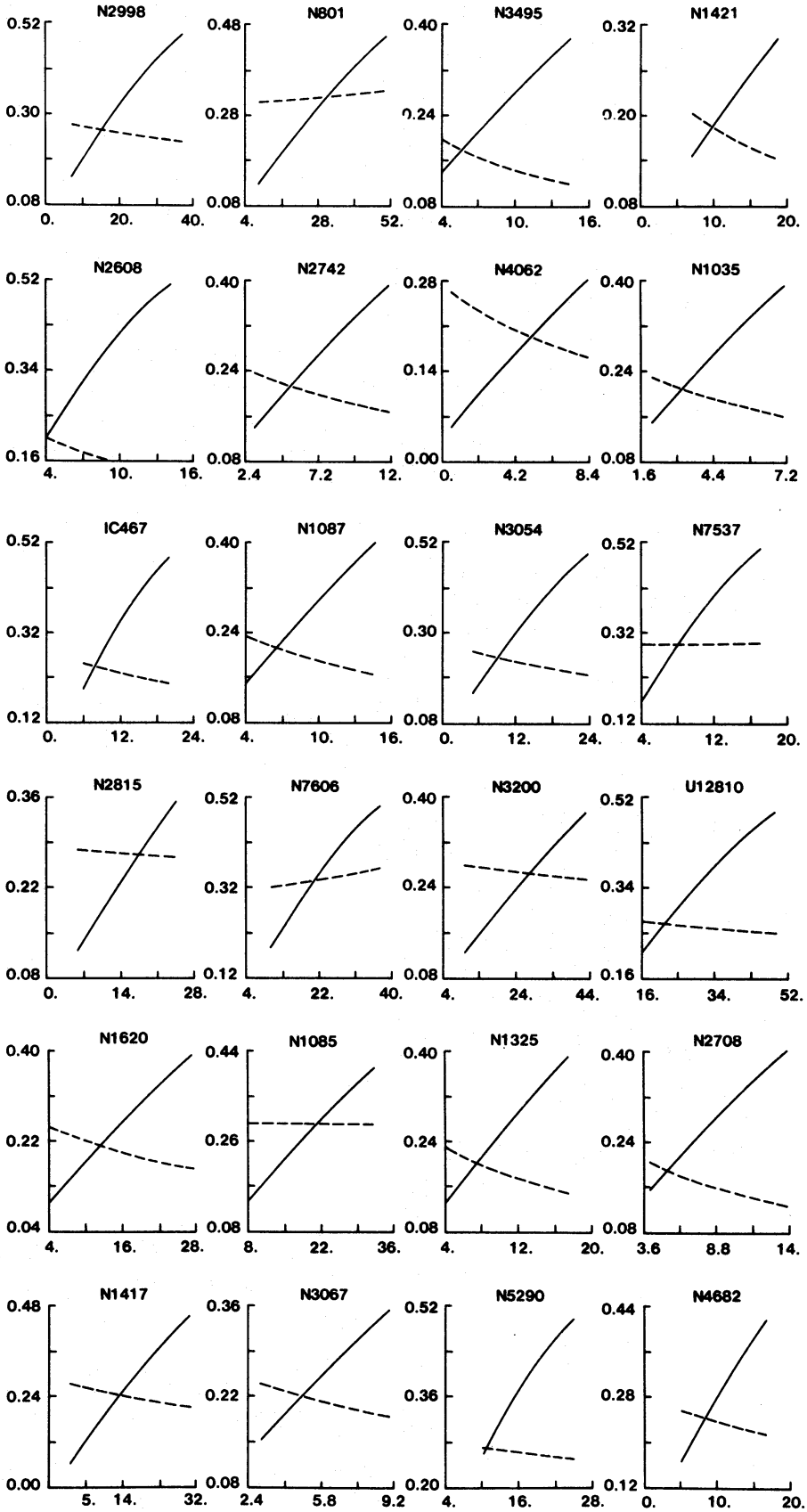


Figure 2. $a(R) \equiv \tilde{V}(R)/V(R)$ (dashed lines) and $a_D(R) \equiv \tilde{V}_{\text{disc}}(R)/V_{\text{disc}}(R)$ (solid lines) plotted as functions of galactocentric radii (in kpc).

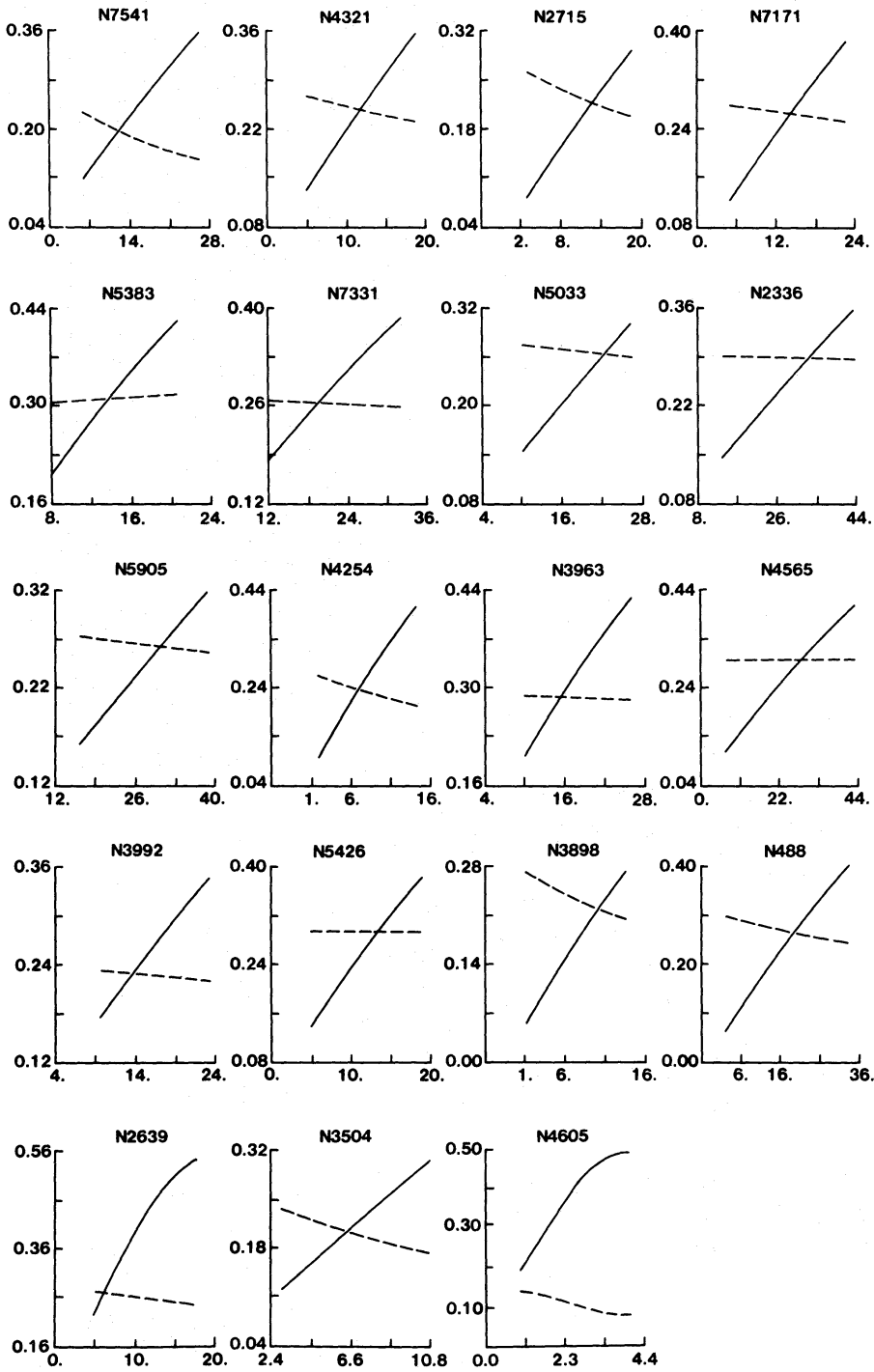


Figure 2—continued

$V_{\text{lum}}^2 = V_{\text{disc}}^2 + V_{\text{bulge}}^2 + V_{\text{halo}}^2$ has a steeper-decreasing profile than V_{disc}^2 , implying that a_{lum} increases even steeper than a_{D} . In these regions the only way to solve the discrepancy between luminous and dynamical velocity profiles then is by allowing the presence of a dark-matter component having $dV_{\text{halo}}^2/dR > 0$. In regions where $a_{\text{D}} < a$ the situation is more open, and a bulge and/or a stellar halo could be invoked to eliminate it.

In Fig. 3 we plot the critical radius R_{C} , marking the boundary of the ‘twilight zone’ in which dark

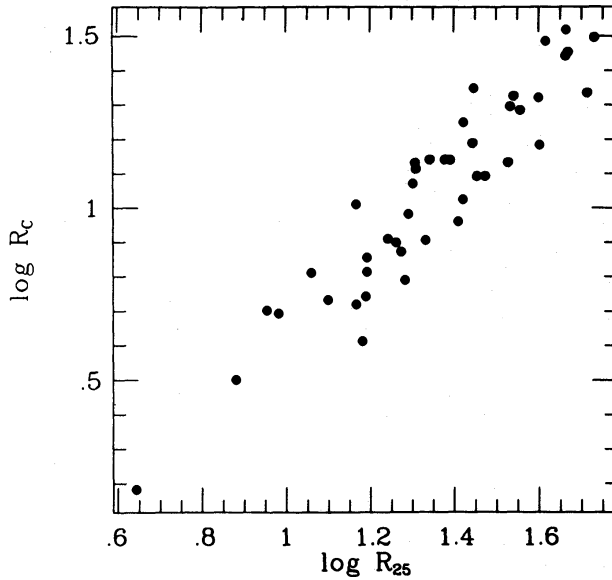


Figure 3. Critical radius R_C such that for $R > R_C$ a dark component is required. Notice that for $R_{25} = 4$ kpc it is $R_C/R_{25} = 0.4$, while for $R_{25} = 60$ kpc it is $R_C/R_{25} = 0.6$.

matter is dynamically required [i.e. $a(R_C) = a_D(R_C)$], as a function of the galaxy isophotal radius R_{25} .

What is the configuration of dark matter? It is very unlikely that dark matter may reside in the disc itself. In fact, if dark matter is constituted by dissipationless particles, it is virtually impossible to confine it in a thin disc-shaped configuration. If, on the contrary, dark matter is baryonic and does reside in the disc, there is no obvious *a priori* reason why it should be distributed so differently from luminous matter in order to generate the observed circular velocity profiles (additional problems arise from careful examination of individual baryonic candidates – Heygi & Olive 1986). There are further observational arguments against the hypothesis of dark matter being arranged in a disc, which positively favour a spherical distribution of the unseen component: (i) in polar-ring S0 galaxies the comparison between disc and polar-ring velocities is consistent with a nearly-spherical dark-matter distribution (Whitmore *et al.* 1987); (ii) in the Galaxy, the value of the ratio between the radial and the z -component of the acceleration in the solar neighbourhood implies that the amount of dark matter needed to justify a flat rotation curve cannot all reside in the disc (Rohlfis 1982); (iii) the spherical distribution of globular clusters around the Galaxy underlies a spherical potential (Frenk & White 1980).

In view of all these arguments we shall henceforth assume that dark matter resides in a spherical halo embedding a thin exponential disc.

4 How much dark matter is there inside the optical size?

The condition for centrifugal equilibrium at R_{25} reads:

$$V_{25}^2 = V_{\text{disc}}^2(R_{25}) + V_{\text{halo}}^2(R_{25}). \quad (13)$$

By derivation of equation (13) we have

$$V_{25} V_1 / R_{25} = V_{\text{disc}}(R_{25}) dV_{\text{disc}}(R_{25})/dR + V_{\text{halo}} dV_{\text{halo}}(R_{25})/dR. \quad (14)$$

Let us define

$$a_h = 1 - 1/\sqrt{2(1 + d \log V_{\text{halo}}/d \log R)^{1/2}} \quad (15)$$

and

$$\theta = V_{\text{disc}}^2(R_{25})/V_{\text{halo}}^2(R_{25}). \quad (16)$$

Then from equations (11)–(16) we get

$$\theta = \frac{[1 - a_{\text{h}}(R_{25})]^2 - [1 - a(R_{25})]^2}{[1 - a(R_{25})]^2 - [1 - a_{\text{D}}(R_{25})]^2}. \quad (17)$$

Let

$$\beta \equiv \frac{\mathcal{M}_{\text{disc}}(R_{25})}{\mathcal{M}_{\text{halo}}(R_{25}) + \mathcal{M}_{\text{disc}}(R_{25})}$$

be the ratio between the disc mass and the total mass inside the optical size. Then:

$$\beta = \frac{\theta}{R_{25}/R_{\text{D}}F(R_{25}/R_{\text{D}}) + \theta}, \quad (18)$$

where for simplicity we have assumed $\mathcal{M}_{\text{disc}}(R_{25}) \approx \mathcal{M}_{\text{D}}$. Were this not the case, we should substitute $\theta \rightarrow \theta[1 - (1 + R_{25}/R_{\text{D}})\exp(-R_{25}/R_{\text{D}})]$. Thus $\beta = \beta[a(R_{25}), R_{25}/R_{\text{D}}, a_{\text{h}}(R_{25})]$, being $a(R_{25})$ and R_{25}/R_{D} observed while $a_{\text{h}}(R_{25})$ is *a priori* unknown unless a dark-matter density distribution is assumed.

The crucial points are: (i) β has a much weaker dependence on $a_{\text{h}}(R_{25})$ than on $a(R_{25})$, and (ii) we can successfully exploit this piece of evidence in solving the galaxy structure.

In order to prove the first statement we start out by realizing that, since for the great majority of galaxies $0.2 \leq \theta \leq 2$ as indicated by the dynamical-to-visible mass ratios (Fig. 1 and equation 10), equations (18) and (17) imply that, typically,

$$\partial\beta/\partial a_{\text{h}}/\partial\beta/\partial a \leq 0.3 \quad (19)$$

where all quantities are evaluated at R_{25} . Furthermore, we can estimate the maximum and minimum values of $a_{\text{h}}(R_{25})$ which are allowed in each galaxy from the observed density distributions of total and visible matter. Such values refer, respectively, to the cases where the disc has the minimum and the maximum allowed masses. We define the maximum disc mass as the largest disc mass meeting the following conditions:

(i) kinetic energy must be non-negative: $V_{\text{halo}}^2(R) \geq 0$, then

$$\mathcal{M}_{\text{d max}} \leq V^2(R)R_{\text{D}}/[GF(x)] \quad (20)$$

(ii) halo density must be non-negative: $\rho_{\text{halo}}(R) \geq 0$, then

$$\mathcal{M}_{\text{d max}} \leq (V_0 + V_1 R/R_{25})(V_0 + 3V_1 R/R_{25})R_{\text{D}}/[gH(x)] \quad (21)$$

where $H(x) = x^3[1.5I_0K_0 - 0.5I_1K_1 + 0.5x(I_0K_1 - I_1K_0)]$ and the Bessel functions are evaluated at $x/2$.

Before proceeding further, it is important to comment on the second constraint. In disequality (21) the values of local properties in the innermost regions, i.e. for $R \sim R_1$, strongly constrain the maximum allowed mass. However, both model (7) of the circular velocity and the surface luminosity density (1) might be, to this purpose, a poor approximation to the actual galactic properties in the neighbourhood of R_1 . In particular:

(i) In our model of the circular velocity field we have neglected details of how the circular velocity settles into a straight line starting from $R \sim R_1$. These details, although irrelevant to the determination of the mean gradient, are of crucial importance to the above constraint.

(ii) In such innermost regions the exponential thin-disc model might inadequately describe the disc-matter distribution, so that disequality (21) could no longer be valid unless the actual disc density distribution were substituted.

With these caveats we get for each sample galaxy an estimate of \mathcal{M}_d^{\max} from equations (18) and (20) and of \mathcal{M}_d^{\min} from equation (10). These two mass estimates constrain the distribution of dark matter. In fact, by means of equation (17) we obtain for each galaxy the corresponding $a_{\text{halo}}^{\min}(R_{25})$ and $a_{\text{halo}}^{\max}(R_{25})$ (see Table 2),

$$a_{\text{halo}}^{\min} = 1 - \left[\theta_{\max} \{ [1 - a(R_{25})]^2 - [1 - a_D(R_{25})]^2 \} + [1 - a(R_{25})]^2 \right]^{1/2},$$

$$a_{\text{halo}}^{\max} = 1 - \left[\theta_{\min} \{ [1 - a(R_{25})]^2 - [1 - a_D(R_{25})]^2 \} + [1 - a(R_{25})]^2 \right]^{1/2}. \quad (22)$$

Thus, we estimate $\Delta a_h \sim 1/2 \Delta a$, where Δa_h is the uncertainty on $a_h(R_{25})$, while Δa is the observed range in a ($\Delta a \sim 0.20$). Finally, we obtain the result anticipated above:

$$a_h \partial \beta / \partial a_h \Delta a_h / a_h \ll a \partial \beta / \partial a \Delta a / a. \quad (23)$$

This result allows us to assume, for the purpose of working out disc and halo integral properties, $a_h(R_{25})$ to be constant along the luminosity sequence of galaxies. Also, it provides a tool to estimate the maximum error involved with such an assumption.

The next step is to use the simple idea that galaxy luminosities must correlate with disc dynamical masses, in that both are a measure of the same mass. Then, we find out the ‘typical’ value $a_h^i(R_{25})$ by forcing the $L_B - \mathcal{M}_{\text{disc}}$ relation to minimum scatter. We find (see Fig. 4):

$$a_h^i(R_{25}) = 0.05 \pm 0.03. \quad (24)$$

Table 2. Maximum and minimum values for $a_h(R_{25})$. In cases where the value of $a_h^{\min}(R_{25})$ is reported as 0.000, our method could not formally give a lower constraint to $a_h(R_{25})$.

Object	$a_{\text{halo}}^{\text{MAX}}(R_{25})$	$a_{\text{halo}}^{\text{MIN}}(R_{25})$	Object	$a_{\text{halo}}^{\text{MAX}}(R_{25})$	$a_{\text{halo}}^{\text{MIN}}(R_{25})$
N 2998	0.160	0.097	N 3067	0.088	0.000
N 4605	0.034	0.000	N 5290	0.117	0.041
N 801	0.249	0.172	N 4682	0.122	0.040
N 3495	0.055	0.000	N 7541	0.069	0.000
N 1421	0.086	0.000	N 4321	0.119	0.023
N 2608	0.076	0.028	N 2715	0.107	0.000
N 2742	0.079	0.000	N 7171	0.124	0.056
N 4062	0.098	0.000	N 5383	0.229	0.150
N 1035	0.075	0.000	N 7331	0.148	0.052
IC 467	0.134	0.068	N 5033	0.204	0.120
N 1087	0.078	0.001	N 2336	0.220	0.123
N 3054	0.138	0.073	N 5905	0.216	0.090
N 7537	0.218	0.148	N 4254	0.108	0.025
N 2815	0.166	0.079	N 3963	0.187	0.101
N 7606	0.286	0.218	N 4565	0.199	0.114
N 3200	0.110	0.059	N 3992	0.103	0.000
U12810	0.165	0.090	N 5426	0.205	0.125
N 1620	0.075	0.000	N 3898	0.124	0.000
N 1085	0.195	0.111	N 488	0.145	0.062
N 1325	0.069	0.000	N 2639	0.185	0.130
N 2708	0.060	0.000	N 3504	0.081	0.000
N 1417	0.130	0.060			

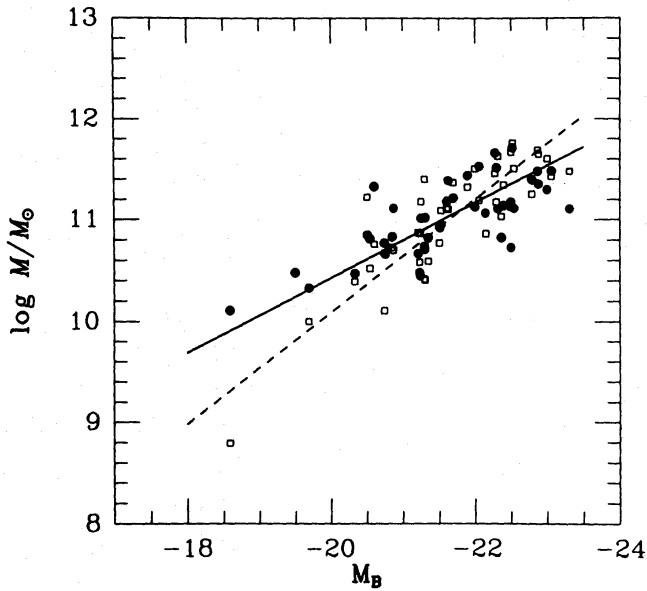


Figure 4. The amount of dark matter (circles, solid line) and disc matter (squares, dashed line) within the optical radius as a function of luminosity.

It is now worth while to discuss our method in terms of the balance between equations and unknowns. For a sample of N objects the problems of mass decomposition has $3N$ unknowns [e.g. \mathcal{M}_D , \mathcal{M}_H and $(d\mathcal{M}_h/dR)_{R_{25}}$ for each galaxy]. Relations (13) and (14) provide us with $2N$ equations. Inequality (23) drops $N-1$ unknowns and (24) provides the last needed equation. Our method, unlike those involving quadratures, has the same number of (approximated)

Table 3. Disc-to-total mass ratios with their uncertainties and disc masses (in solar-mass units).

Object	$\beta \mp \Delta\beta$	M_D	Object	$\beta \mp \Delta\beta$	M_D
N 2998	0.41 \mp 0.06	0.18E+12	N 3067	0.40 \mp 0.08	0.25E+11
N 4605	0.04 \mp 0.03	0.62E+09	N 5290	0.45 \mp 0.06	0.13E+12
N 801	0.68 \mp 0.04	0.30E+12	N 4682	0.41 \mp 0.07	0.53E+11
N 3495	0.17 \mp 0.09	0.25E+11	N 7541	0.27 \mp 0.09	0.15E+12
N 1421	0.30 \mp 0.11	0.73E+11	N 4321	0.52 \mp 0.06	0.12E+12
N 2608	0.17 \mp 0.07	0.13E+11	N 2715	0.52 \mp 0.09	0.74E+11
N 2742	0.30 \mp 0.09	0.33E+11	N 7171	0.55 \mp 0.05	0.15E+12
N 4062	0.39 \mp 0.10	0.30E+11	N 5383	0.69 \mp 0.04	0.13E+12
N 1035	0.28 \mp 0.08	0.10E+11	N 7331	0.57 \mp 0.06	0.22E+12
IC 467	0.36 \mp 0.06	0.39E+11	N 5033	0.77 \mp 0.05	0.25E+12
N 1087	0.29 \mp 0.09	0.26E+11	N 2336	0.71 \mp 0.05	0.46E+12
N 3054	0.33 \mp 0.07	0.13E+12	N 5905	0.70 \mp 0.06	0.42E+12
N 7537	0.55 \mp 0.05	0.38E+11	N 4254	0.38 \mp 0.07	0.59E+11
N 2815	0.65 \mp 0.05	0.32E+12	N 3963	0.59 \mp 0.05	0.11E+12
N 7606	0.70 \mp 0.03	0.32E+12	N 4565	0.64 \mp 0.05	0.40E+12
N 3200	0.57 \mp 0.05	0.49E+12	N 3992	0.52 \mp 0.07	0.23E+12
U12810	0.45 \mp 0.06	0.27E+12	N 5426	0.68 \mp 0.03	0.73E+11
N 1620	0.28 \mp 0.08	0.15E+12	N 3898	0.59 \mp 0.09	0.17E+12
N 1085	0.63 \mp 0.05	0.44E+12	N 488	0.49 \mp 0.06	0.57E+12
N 1325	0.25 \mp 0.09	0.50E+11	N 2639	0.43 \mp 0.06	0.21E+12
N 2708	0.19 \mp 0.08	0.57E+11	N 3504	0.41 \mp 0.10	0.46E+11
N 1417	0.37 \mp 0.06	0.29E+12			

equations as unknowns. In Table 3 we show the obtained values of β and their uncertainties computed for each galaxy by means of equations (18) and (22), and the respective disc masses. The reported uncertainties do not take into account any errors propagated from observable quantities but only refer to the maximum theoretical error inherent in our method (the observational errors are generally very small for sample C. We recall that our strategy is concerned with the theoretical uncertainties attached to dark matter rather than with observational errors, which in principle can be reduced).

5 Galactic discs: masses, luminosities, sizes and colours

In Fig. 5(a) we plot β as function of luminosity. It is readily realized that the dynamical importance of dark matter within the disc regions is differential with luminosity, i.e. it depends on the amount of visible matter. In excellent agreement with the trend shown by the (dynamical mass)-to-light ratios (Fig. 1), within their respective optical sizes fainter ($M_B = -19$) galaxies have

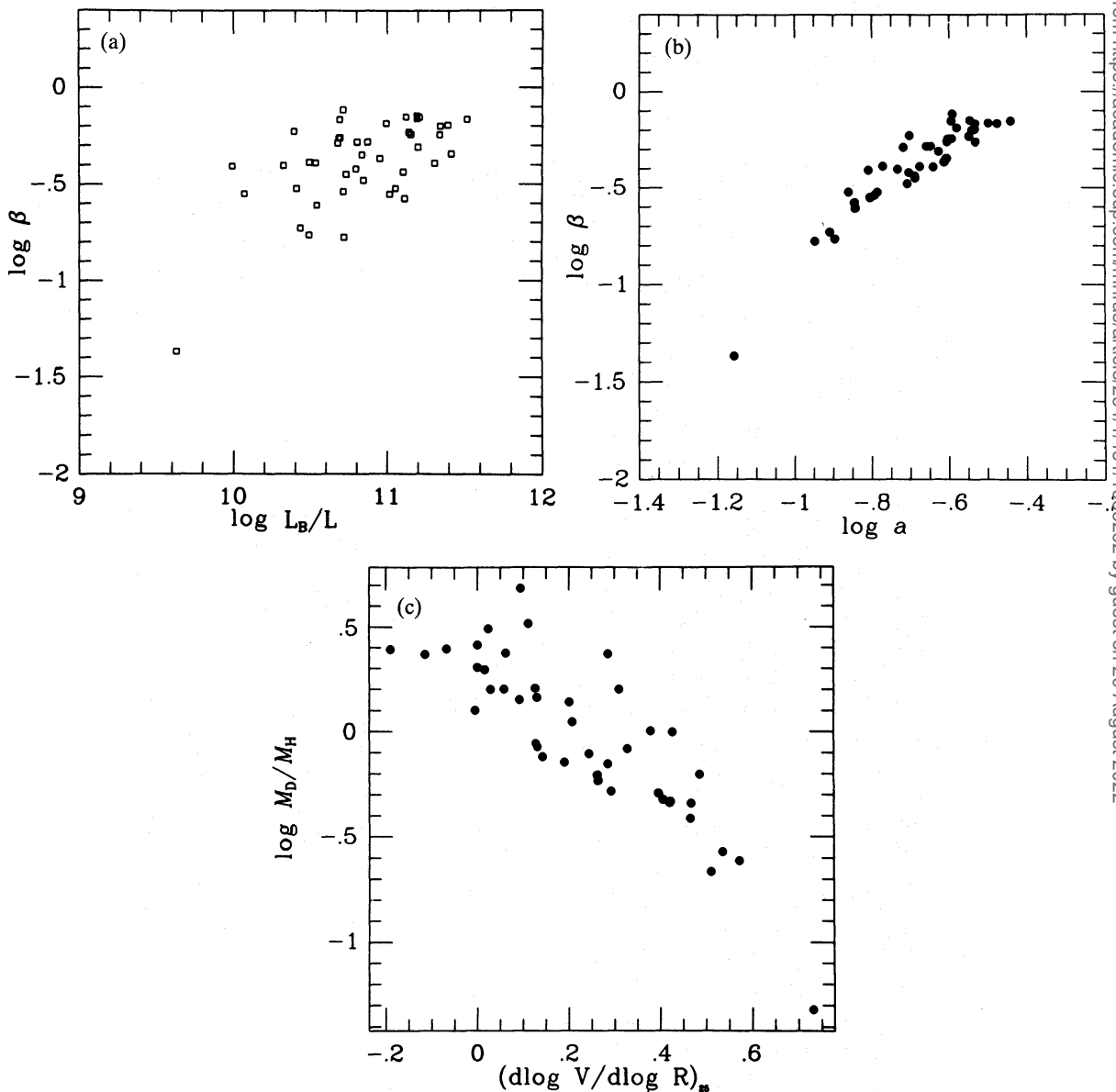


Figure 5. (a) Computed disc-to-total mass ratios β as a function of luminosity. (b) β as a function of the mean-velocity-gradient indicator a . (c) Disc-to-halo mass ratio as a function of the logarithmic gradient of velocity fields.

a larger dark-mass fraction, $\beta \approx 0.2$, while brighter ($M_B = -23$) galaxies show a smaller dark-mass fraction, $\beta \approx 0.8$. Quantitatively, we find

$$\begin{aligned} \beta &= 0.5 (L_B / 10^{11} L_\odot)^{0.56} \\ r &= 0.60, \quad N = 43. \end{aligned} \quad (25)$$

Moreover, the visible-to-total mass ratio is imprinted on the (axisymmetric) profile of the rotation curve through the velocity-gradient indicator a (Fig. 5b):

$$\begin{aligned} \beta &= 0.72 (a / 0.29)^{1.6} \\ r &= 0.93, \quad N = 43. \end{aligned} \quad (26)$$

Hence, galaxies with flat rotation curves ($a = 0.29$) have most mass in the visible component ($\beta = 0.70$), while galaxies with steep rotation curves ($a = 0.15$) have a large fractional amount of dark matter even within the optical disc ($\beta = 0.25$) [see also Fig. 5(c)].

An important consequence of equation (25) is that we can understand the physical basis of the empirical Tully–Fisher correlation (hereafter TF) (Tully & Fisher 1977). Using definition (16), the condition (13) for centrifugal equilibrium at R_{25} reads:

$$\mathcal{M}_D = G^{-1} [R_{25}/R_D F(R_{25}/R_D)]^{-1} V_{25}^2 \left(\frac{\theta}{1+\theta} \right) R_{25} \quad (27)$$

where \mathcal{M}_D is the disc mass. As discussed in Section 2, in each galaxy the stellar mass-to-light ratio is found to be constant along the disc and independent of luminosity. Then, from equations (1) and (4) we have

$$L_B \propto R_{25}^2, \quad (28)$$

$$\mathcal{M}_d \propto L_B. \quad (29)$$

The quantity $R_{25}/R_D F(R_{25}/R_D)$ has a small scatter among galaxies, so that it can be considered constant [in our sample $R_{25}/R_D F(R_{25}/R_D) = 1.1 \pm 0.05$]. Then, combining equations (27)–(29) we get

$$L_B \propto V_{25}^4 \lambda \quad (30)$$

with $\lambda = \theta^2 / (1+\theta)^2$ [by comparison with equation (27), notice that $\lambda \approx \beta^2$]. The case $\lambda = 1$ (no dark matter) yields the $L \propto V^4$ result first obtained (by a similar argument) by Aaronson *et al.* (1979). (A power-law relation between luminosity and velocity can also be obtained by a general hypothesis on the structure of protogalaxies and by assuming a constant total \mathcal{M}/L ratio, Burstein & Sarazin 1983.) The important point, however, is that, due to the differential presence of dark matter along the luminosity sequence, λ itself is a function of luminosity (or, alternatively, of the axisymmetric velocity slope):

$$\begin{aligned} \log \lambda &= -(7.38 \pm 0.86) - (0.32 \pm 0.04) M_B, \\ r &= 0.59, \quad N = 43. \end{aligned} \quad (31)$$

It is thus realized from equations (30) and (31) that there exists a theoretical relationship between the luminosity of a galaxy and its maximum circular velocity V_{25} as a physical consequence of the condition for centrifugal equilibrium of a thin stellar disc embedded in a dark spherical halo. Therefore, the $\log L_B - \log V_{25}$ correlation (or $\log L_B - \log V_M$, since most galaxies' rotation curves are either rising or flat) is predicted with a slope not too much different from 4, especially if most galaxies are very bright, hence their β s (and λ s) tend to saturate at 1 [cf. Fig. 5(a)].

We remark that the presence of dark matter in galaxies ranges between 20 and 80 per cent of the total mass encompassed by the optical disc. If random, such a dramatically different presence (see Table 3), would eventually destroy any luminosity–kinematics relation possibly holding for the visible component. This, however, is not the case because the amount of dark matter inside the optical disc is finely modulated with the amount of visible matter, so that a correlation between kinematics (total matter) and luminosity is still possible with a relatively small intrinsic scatter in spite of the strong differential presence of dark matter. Then, as a consequence of this effect, galaxies with magnitude $M_B > -23$ will be fainter by $\Delta M_B \approx 0.8 (M_B + 23)$ mag with respect to the value obtained by extrapolating to lower magnitudes the luminosity–kinematics relation as it is in the neighbourhood of $M_B = -23$.

We can get rid of the presence of dark matter in the luminosity–kinematics relation by correlating luminosity with the visible-matter contribution to V_{25} , V_* , after turning off the (differential) dark-matter contribution to V_{25} . Actually, from equations (30) and (31) we obtain

$$\log V_* = \log V_{25} - 7.9 \times 10^{-2} (M_B + 23). \quad (32)$$

We find:

$$M_B = -(8.9 \pm 1.0) - (5.8 \pm 0.5) \log V_*,$$

$$N=43, \quad r=0.86, \quad \sigma=0.53 \text{ mag}. \quad (33)$$

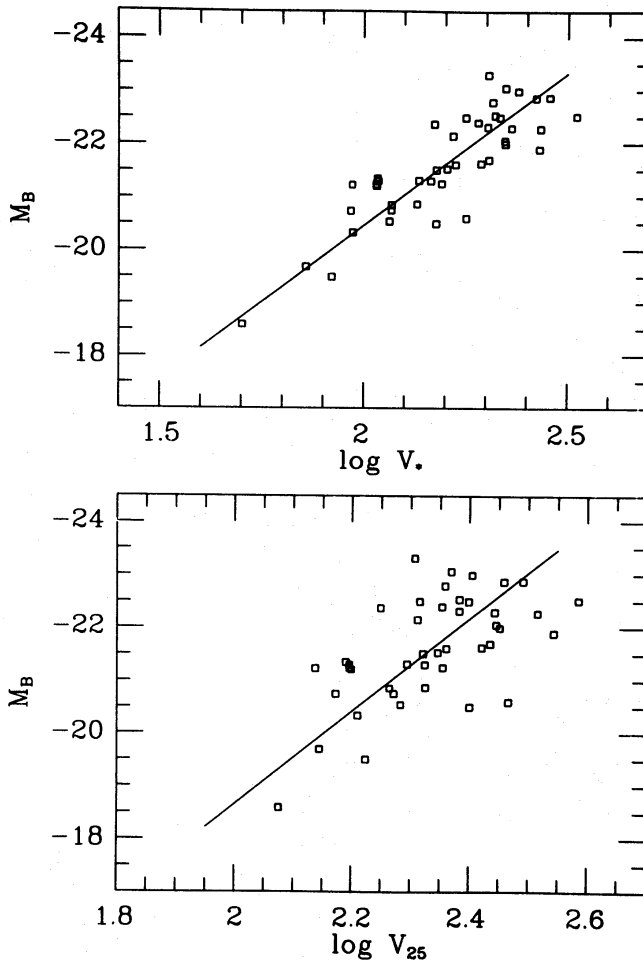


Figure 6. The luminosity–kinematics relation for sample C, before (bottom) and after (top) removing the dark-matter contribution from the maximum velocity.

It is interesting to compare relation (33) with the TF correlation for the sample C,

$$M_B = -(1.1 \pm 2.5) - (8.8 \pm 1.1) \log V_{25},$$

$$N=43, \quad r=0.61, \quad \sigma=0.80 \text{ mag.} \quad (34)$$

From relations (33) and (34) and Fig. 6 one can appreciate the effectiveness of this correction to the TF relation. This can be understood by realizing that in each galaxy the dark-matter contribution to the maximum circular velocity $\approx V_{25}$ depends on the mean rotation-curve slope (or alternatively on luminosity), so that it can be easily taken care of by means of equation (32). Thus, the kinematics–luminosity relation is left with remarkably less scatter, $\Delta\sigma \sim 0.25$ mag, and a unique (flatter) slope over the whole luminosity range.

We wish to stress that, in order to more clearly discuss the physical basis of the TF correlation, in equation (32) we have hidden the explicit dependence of V_* on $a(R_{25})$. Moreover, if we want to work out a new kinematics–luminosity relation as a consequence of basic dynamics, we must also work out the relations $\lambda = \lambda[a(R_{25})]$ and $V_* = V_*[V_{25}, a(R_{25})]$. We find

$$\log V_* = \log V_{25} + 1.64a(R_{25}) - 0.52, \quad (35)$$

which gives (for sample C) exactly the same luminosity–kinematics relation (33) and similar scatter.

It is of crucial importance to test relation (32) in an independent sample of galaxies. To this purpose we study the Aaronson *et al.* sample of galaxies (Aaronson *et al.* 1982), where *H*-mag and corrected 21-cm linewidths are given for 300 Sa–Im galaxies. This sample is particularly useful because it spans a large range in IR magnitudes (~ 7 mag) and still has ~ 40 object mag^{-1} . Moreover the IR band is more likely to be dominated by the old disc population (which contributes to virtually the whole disc mass) than the *B*-band where star-formation bursts of even modest strength might dominate the light (Aaronson *et al.* 1979).

By means of relation (32) we extract the contribution V_* due to visible matter from the 21-cm linewidths. In the correcting term we assume $\langle B-H \rangle = 2.3$ (see Rubin *et al.* 1985) in order to transform IR magnitudes into *B* magnitudes. After the dark-matter contribution has been removed all galaxies pile up on a unique straight line with a slope similar to that of (33), and the scatter is dramatically decreased from 0.70 to 0.36 mag (Fig. 7). This result strongly supports the universal effectiveness of relation (32) in dealing with the presence of dark matter and shows that in samples ranging through 6–7 mag the scatter is dominated by the differential amount of dark matter within the optical disc.

Due to lack of knowledge of the velocity fields of most galaxies in the Aaronson *et al.* sample, we had to use the distance-dependent (through M_B) correction (32) to V_{25} as a hidden parameter. Therefore, we caution that the spectacular decrease of scatter we have obtained by removing the dark-matter contribution might not actually imply such a remarkable improvement in the determination of distances. However, since relation (33) extends to the very faint end of the luminosity function, it makes it possible to use dwarf spirals in the Local Group and beyond as local calibrators.

As a result of the mass decompositions worked out in the previous section, we can compute the stellar mass-to-light ratios for each galaxy of our sample. When compared and plotted versus galaxy colours, they provide information on the age of galaxies, luminosity evolution, star-formation rate and present mass function. We recall that in the previous section we have used stellar-evolution models only in order to estimate the maximum error involved with our mass-decomposition method and to rule out the possibility that flat-rotation-curve galaxies are halo-dominated. Computed disc masses have no bias towards any particular stellar-evolution model and have been obtained without using galaxy colours. Therefore it is worth while to compare the

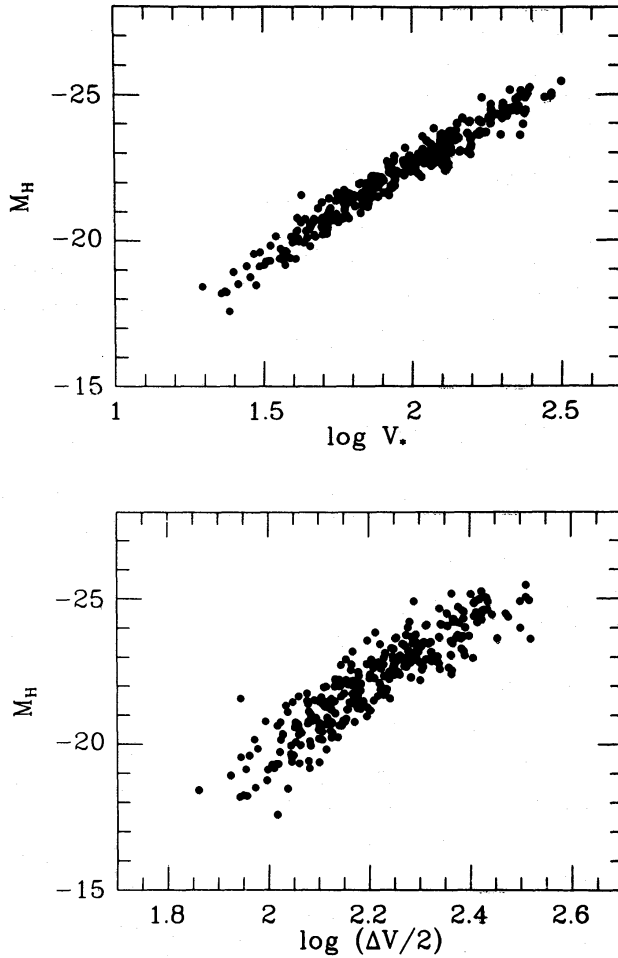


Figure 7. The luminosity–kinematics relation for the Aaronson *et al.* sample, before (bottom) and after (top) the dark-matter contribution has been removed from the maximum velocity. Since for most galaxies in the sample the circular velocity field is not available we estimate the contribution of dark matter by means of relation (32) (see text). In deriving galactic distances we assumed a homogeneous Hubble-flow model. However, the galaxies belonging to a large group in the Geller–Huchra catalogue (1982) have been placed at the group’s mean redshift. We dropped a few galaxies belonging to the Local, Sculptor, CVn and M101 groups for which the homogeneous-flow model is not applicable. Eventually 290 objects are left.

observed mass-to-light versus colour relation with the analogous relation predicted by the models.

Tinsley (1981), by comparing (dynamical mass)-to-light ratios with the ones predicted for the observed colours, found that bluer galaxies have comparatively more dark matter than redder galaxies. We can now address this topic, having an effective way to decompose the dynamical mass into a visible and a dark component, so that we can actually compare the disc mass-to-light ratios with galaxy colours. We find

$$\log (\mathcal{M}_D/L_B) = -(1.1 \pm 0.2) + (2.3 \pm 0.3)(B-V) + \log (H_0/50). \quad (36)$$

First, we understand the dark-matter contamination on the $(\mathcal{M}_{\text{dyn}}/L_B)-(B-V)$ relation as the effect of a differential presence of dark matter along the luminosity sequence. Fainter (and bluer in the Tinsley sample) galaxies have relatively more dark matter than brighter (and redder) ones. (Note that the colour–magnitude relation present in the Tinsley sample might be partially due to a mix of local faint irregular galaxies with bright spirals whose distances are obtained from

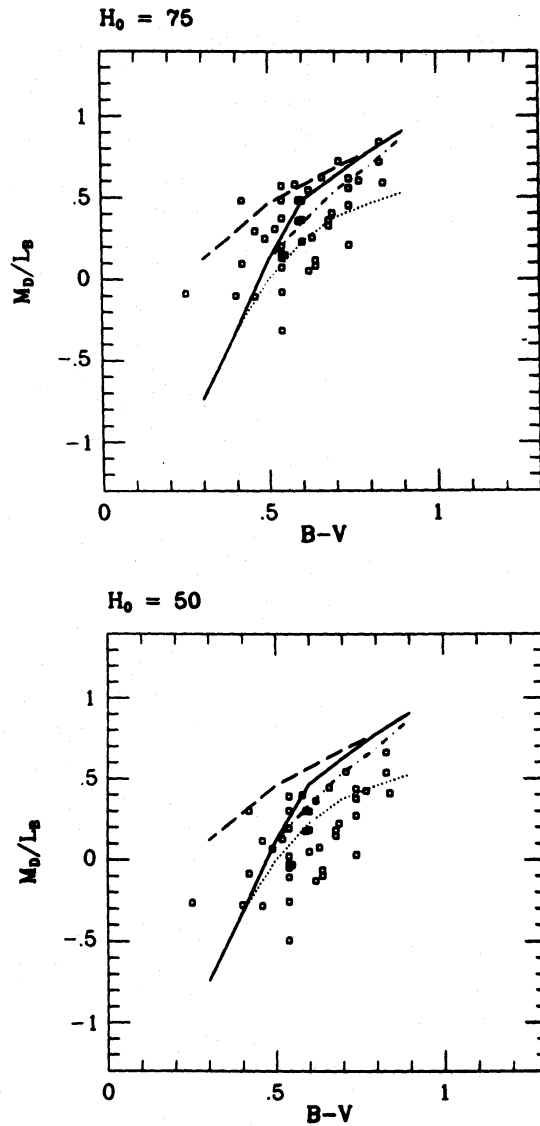


Figure 8. Disc mass-to-light ratios versus colours for sample C, computed assuming $H_0=75$ (top) and 50 (bottom) $\text{km s}^{-1} \text{Mpc}^{-1}$. Theoretical predictions of LT evolutionary models are also plotted: a solid line refers to the 10-Gyr continuous-SFR model, a dash-dotted line to the 10-Gyr exponentially-decreasing-SFR model, a dotted line to the 5-Gyr continuous-SFR model, and a dashed line to the 1-Gyr-burst red-disc model. (Mass-to-light ratios are in decimal logarithm).

redshifts.) When this contamination is bypassed by directly relating disc mass-to-light ratios to colours we conclude (see Fig. 8) that:

- (i) Stellar-evolution models are able, at least as a first approximation, to describe 10 Gyr of disc evolution and explain the observed colours of galactic discs.
- (ii) The best agreement on the zero-point value between theoretical models and observations is for $H_0 \sim 75 \text{ km s}^{-1} \text{Mpc}^{-1}$. However, at this stage, higher and lower values for H_0 cannot be ruled out.
- (iii) A number of galaxies seem to undergo a burst phase. The strengths of such bursts indicate a correlation with colours suggestive of a LT 1-Gyr-burst red-disc model.

All these results, although requiring a much larger sample for confirmation, are of crucial

importance to investigating the problems of galaxy luminosity evolution, number counts and searches for primeval galaxies.

The above conclusions are concerned with the qualitative comparison between theory and observation. However, we think that, once any halo contribution is eliminated, it is also possible to undertake a quantitative study of the luminosity evolution of galaxies, in terms of their stellar content. Obviously this project would require more objects in different bands and flexible evolutionary models in order to be able to obtain quantitatively useful results.

6 Discussion

At this point it seems appropriate to discuss the results so far obtained and the merits of the method used.

First, we discuss the maximum-disc hypothesis (MDH). Such a hypothesis assumes that in the inner regions of a galaxy dynamics are dominated by disc matter (Carignan & Freeman 1985; van Albada & Sancisi 1986; Kent 1986). Then, via an assumed halo-density distribution (usually a pseudo-isothermal distribution with central density and core radius as free parameters), the basic halo properties and the disc \mathcal{M}/L_B ratio are worked out by fitting the difference between the observed rotation curve and the curve generated by the visible matter (usually an exponential thin disc).

In spite of its promising simplicity, however, several arguments indicate that the application of MDH requires caution, and that its results should be considered as a constraint to the maximum allowed value for the disc mass-to-light ratio rather than a working procedure for dark versus visible mass decomposition. In fact:

(i) Even if we assume that the dark mass is negligible in the innermost regions of galaxies, in many cases the bulge mass is not negligible there. In principle it is possible to account for the bulge mass by means of a bulge-mass model derived from the luminosity distribution with the value of $(\mathcal{M}/L)_{\text{bulge}}$ as a free parameter. Nevertheless this approach seems to bring unnecessary complications, which arise from the inappropriate comparison of dynamical versus visible masses in the inner regions of galaxies rather than at the limit of the optical disc. In fact, some difficulties are immediately apparent when MDH is applied to a large sample of galaxies (Kent 1986; most of the 37 galaxies studied in that paper also belong to the sample used in the present work): in a few cases non-physical solutions are found, in several (12) other cases the disc mass-to-light ratios exceed (even by a factor of 5) the respective bulge mass-to-light ratios, implying a large amount of disc dark (unseen) matter.

(ii) Let us now consider faint spirals (approximately 40 per cent of the galaxies in Table 1). Since a dramatic discrepancy between the respective typical profiles of observed and disc-generated rotation curves is already apparent in the galaxies' innermost regions (see Section 2), the hypothesis that the amount of dark matter is negligible there can hardly be maintained for those systems.

Moreover, we emphasize that our method for deriving halo and disc properties is not biased against MDH at all. Our method is completely transparent to MDH so that MDH can be effectively tested by our procedure.

According to our results, MDH might be considered as a working hypothesis for luminous, large galaxies, because the fractional amount of dark matter within the optical size is relatively small in those systems. On the contrary, our results are strongly opposed to MDH in the case of faint, small galaxies, whose dynamics are actually found to be halo-dominated. We think that in the case of faint galaxies ($M_B > -20$) MDH sets only a limit to the maximum disc mass which is dynamically allowed.

There are several independent arguments that support our picture:

(i) Direct measurements of the flattening of the equipotential surfaces in three polar-ring S0 galaxies at $R \sim 0.6 R_{25}$ (i.e. ~ 2 length scales) show that even in the inner regions a dark spherical halo is found to be the dominant mass component (Whitmore *et al.* 1987). Moreover, if the visible-to-dark mass ratio is inferred by means of the scale-free gravitational potential of Monet *et al.* (1981), we also quantitatively agree with their results, $\beta \approx 0.1$ for galaxies of luminosity $M_B \approx -20$.

(ii) Evidence that faint galaxies are dynamically dominated by haloes comes also from the other branch of the Hubble sequence. Comte (1984), analysing a sample of irregular and Magellanic-like galaxies, finds that most of them are halo-dominated ($\beta \approx 0.1$).

(iii) Here we discuss again the results of our analysis of the infrared version of the TF correlation. This luminosity versus maximum circular velocity relation shows the interesting feature that its slope is steeper for low-luminosity galaxies. Such a steepening systematically decreases towards higher luminosities and only asymptotically approaches the value 10 for high-luminosity objects. This feature fits perfectly into our picture. According to the results of our method, only very luminous galaxies contain an actually negligible fraction of dark matter inside their optical size, so that the TF slope of 10 is reached only at the very bright end of the luminosity sequence. On the contrary, in fainter galaxies a larger fraction of the dynamical mass inside the disc size is due to non-luminous matter, so that dimmer galaxies will actually be less luminous than one might expect by extrapolating from the behaviour of brighter galaxies. Thus a steepening will result in the TF relation at lower luminosities. The differential presence of dark matter, therefore, will produce the actually observed curvature of the TF correlation. When the dark-matter contribution is taken away from the maximum velocity, the effect disappears and consequently the scatter drops by a factor of 2.

We conclude this section by discussing the possibility of a constant value of the visible-to-dark mass ratio in all galaxies independently of their properties. This possibility has been explicitly claimed or has been often used as a working hypothesis (for example in theories of galaxy formation which assume that the formation of spirals can be understood by studying the formation of a 'typical' spiral), so that a careful discussion of this point is appropriate.

We have found (see Section 5) a large systematic change of the dynamical importance of dark matter along the luminosity sequence, which rules out the case that spiral galaxies may have the same dark-mass fraction within the optical disc. Two further immediate objects stand against such a case:

(i) Let us consider galaxies of the same Hubble type (for example Sc galaxies in order to also avoid problems connected with the bulge component). All galaxies have the same disc mass distribution $\mathcal{M}_{\text{disc}}(R/R_D) \sim [1 - (1 + R/R_D) \exp(-R/R_D)]$ (in radial units of R_D). However, the profiles of rotation curves show that the total mass distribution $\sim V^2 R$ changes dramatically from galaxy to galaxy. For example, in NGC 801 it is $\mathcal{M}_{\text{dyn}}(R/R_D) \sim R/R_D$, while in NGC 4605 it is $\mathcal{M}_{\text{dyn}}(R/R_D) \sim (1 + R/R_D)^2 R/R_D$. Such a discrepancy could be explained only in terms of substantial differences in the dark-matter mass distribution. Moreover, since we can exclude that large galaxies like NGC 801 are halo-dominated (see Fig. 1), we are forced to the conclusion that such differences in the density distribution of total matter imply substantial differences in the fractional amount of dark matter.

(ii) If the dark-mass fraction inside R_{25} were approximately constant among galaxies, the knowledge of the whole velocity fields would not improve the luminosity–kinematics relation but would simply shift its zero-point. Therefore, the case that we have been able to build up, on a totally empirical and model-independent basis, a substantially improved luminosity–kinematics

relation by using the whole information of the circular velocity fields (Paper I), strongly indicates a systematic, differential importance of the presence of the dark component.

The above arguments, therefore, call for disc-formation theories in which the present fractional amount of dark matter, frozen in the shape of rotation curves, is a quantity crucial to describing both the present structure and the past dynamical evolution of spiral galaxies (e.g. see Davis *et al.* 1985).

7 Conclusions

In this paper we have worked out some physically relevant properties of spiral galaxies in order to obtain a more detailed knowledge of their structural properties. We tackled this fundamental problem by using the following strategy:

- (i) We are interested in very general, basic, recurring properties of spirals, hence we neglected any occasional, peculiar feature.
- (ii) We do not work out integral properties as a by-product of an analysis which strongly relies on unknown properties of dark matter or on quantities which are supposedly little connected with the mass-discrepancy problem. Rather, we develop a method whose aim is precisely to obtain the integral properties of galaxies from the directly observed ones. Our method provides no information on local properties of dark matter.

To this purpose, we used all suitable published data (43 galaxies with both good photometry and rotation curves) to build up a sample which encompasses galaxies ranging through 4–5 mag in blue luminosity with available velocity fields and exponential-disc length-scales. Then we worked out the respective halo-to-disc mass ratios inside the optical discs as a function of the logarithmic gradients of visible, total and dark matter. The latter dependence proved weak, so that, within a reasonably small uncertainty, we have been able to decompose the disc and halo masses from the dynamical mass $G^{-1}V_{25}^2R_{25}$ in each galaxy of the sample.

The values we find show the ubiquitous presence of dark matter in each galaxy. In fact, there is a critical radius R_C such that for $R > R_C$ the observed mass distributions of total and visible matter strongly imply the presence of dark matter (i.e. of an unseen component with a density distribution decreasing less than R^{-2}).

The ratio between visible and dark masses at the optical edge R_{25} varies according to the galaxy's luminosity. The luminosity sequence actually turns out to be a dark-to-visible mass-ratio sequence. Faint galaxies are halo-dominated even in the disc regions ($\mathcal{M}_{\text{disc}}/\mathcal{M}_{\text{halo}} \sim 0.2$), while the disc dominates the optical dynamics of bright galaxies ($\mathcal{M}_{\text{disc}}/\mathcal{M}_{\text{halo}} \sim 4$).

This result leads us to explain the Tully–Fisher correlation as connected with the condition for centrifugal equilibrium of a self-gravitating exponential thin disc embedded in a spherical halo. The presence of dark matter does not destroy the kinematics–luminosity relation which holds for visible matter, because its fractional amount is modulated by luminosity. Then, the Tully–Fisher correlation is theoretically justified, provided that an additional parameter is introduced, i.e. the mean slope of the rotation curve or a predicted function of luminosity. Such an additional parameter physically acts as a tool to remove the dark-matter contribution from the maximum circular velocity.

By analysing our sample and the IR sample of galaxies by Aaronson *et al.* (1982), we have shown that the theoretically suggested luminosity–kinematics relation is a significant improvement over the conventional Tully–Fisher correlation. Such a relation, unlike the TF, spans through 7 mag with no change of slope. Moreover its scatter is remarkably small ($\sigma = 0.53$ mag for our sample and 0.36 mag for the Aaronson *et al.* sample) and considerably reduced compared with the TF (by $\Delta\sigma = 0.27$ and 0.34 mag respectively).

By the knowledge of disc masses (decomposed from dynamical masses) and of colours we are able to compare the ‘observed’ $(\mathcal{M}/L_B)_{\text{disc}} - (B-V)$ relation with the stellar-evolution models’ predictions. We find that the ‘observed’ $(\mathcal{M}/L_B)_{\text{disc}}$ ratios are able to explain the observed colours of spiral galaxies in a scenario involving continuous star formation for ~ 10 Gyr and $H_0 \sim 75 \text{ km s}^{-1} \text{ Mpc}^{-1}$.

We would like to conclude this paper by outlining an observational program which in our opinion would be extremely useful and clarifying.

(i) Faint galaxies seems to be very interesting objects. Their dynamics is completely dominated by their dark haloes, so that it may be possible to investigate also some local properties of halo matter. Unfortunately, there are very few non-local objects in the magnitude range $-17 \geq M_B \geq 20$ with measured rotation curves. Therefore, we suggest that it would be of considerable interest to focus observations on low-luminosity normal spiral galaxies.

(ii) Quite surprisingly, for a sizeable fraction of galaxies with high-quality extended rotation curves there is no colour-fledged photometry. In particular, the $(B-V)$, $(B-I)$ and $(U-B)$ colours are available for about 65, 30 and 30 per cent of the galaxies of our sample respectively. Multicolour information is even scarcer (< 20 per cent of galaxies with observed kinematics have $UBVRI$ colours) and consequently even more badly needed, in that it can provide a potentially crucial help to understand the dynamical and stellar-population evolution of spiral galaxies.

Acknowledgments

It is a pleasure to thank Dennis Sciama for introducing us to this subject and for many suggestions that have considerably improved this work. PS also wishes to thank him for his continuous guidance and help in the supervision of his PhD project. We have greatly benefited from numerous discussions with E. Boldt, L. Danese, G. De Zotti, C. Frenk, G. Palumbo, V. Rubin and S. White. We are grateful to M. Dubal, J. Felten, R. Kelley and A. Szymkowiak for useful comments at various stages during the preparation of the paper. MP wishes to thank, S. Holt for the warm hospitality and the intellectually stimulating environment enjoyed at the Laboratory for High Energy Astrophysics at the Goddard Space Flight Center, Greenbelt, where part of the work was carried out.

References

- Aaronson, M., Huchra, J. & Mould, J., 1979. *Astrophys. J.*, **229**, 1.
 Aaronson, M., Huchra, J., Mould, J., Tully, R. B., Fisher, J. R., van Woerden, H., Goss, W. M., Chamaraux, P., Mebold, U., Siegman, B., Berriman, G. & Persson, S. E., 1982. *Astrophys. J. Suppl.*, **50**, 241.
 Bahcall, J. N., Schmidt, M. & Soneira, R. M., 1983. *Astrophys. J.*, **265**, 730.
 Bahcall, J. N. & Casertano, S., 1985. *Astrophys. J.*, **300**, L35.
 Blackman, C. P., 1982. *Mon. Not. R. astr. Soc.*, **200**, 407.
 Blackman, C. P. & van Moorsel, G. A., 1984. *Mon. Not. R. astr. Soc.*, **208**, 91.
 Blumenthal, G. R., Faber, S. M., Flores, R. & Primack, J. R., 1986. *Astrophys. J.*, **301**, 27.
 Boroson, T., 1981. *Astrophys. J. Suppl.*, **46**, 177.
 Bosma, A., 1981. *Astr. J.*, **86**, 1825.
 Burstein, D. & Rubin, V. C., 1985. *Astrophys. J.*, **286**, 423.
 Burstein, D. & Sarazin, C. L., 1983. *Astrophys. J.*, **264**, 427.
 Carignan, C. & Freeman, K. C., 1985. *Astrophys. J.*, **294**, 494.
 Chincarini, G. & de Souza, R., 1985. *Astr. Astrophys.*, **153**, 218.
 Comte, G., 1984. *Lec. Notes Phys.*, **232**, 170.
 Davis, M., Efstathiou, G., Frenk, C. & White, S. D. M., 1985. *Astrophys. J.*, **292**, 371.
 de Vaucouleurs, G. & de Vaucouleurs, A., 1972. *Mem. R. astr. Soc.*, **77**, 1.
 de Vaucouleurs, G., de Vaucouleurs, A. & Corwin, H. G., 1976. *Second Reference Catalogue of Bright Galaxies*, University of Texas Press, Austin, Texas.

- Elmegreen, B. G. & Elmegreen, D. M., 1985. *Astrophys. J.*, **288**, 438.
- Elmegreen, D. M. & Elmegreen, B. G., 1984. *Astrophys. J. Suppl. Ser.*, **54**, 127.
- Freeman, K. C., 1970. *Astrophys. J.*, **160**, 811.
- Frenk, C. S. & White, S. D. M., 1980. *Mon. Not. R. astr. Soc.*, **193**, 295.
- Geller, M. J. & Huchra, J. P., 1982. *Astrophys. J. Suppl. Ser.*, **54**, 442.
- Gottesman, S. T., Ball, R., Hunter, J. H. & Huntley, J. M., 1984. *Astrophys. J.*, **286**, 471.
- Grosbol, P. J., 1985. *Astr. Astrophys. Suppl. Ser.*, **60**, 261.
- Griersmith, D., 1980. *Astr. J.*, **85**, 1135.
- Hamabe, M., 1982. *Publs astr. Soc. Japan*, **34**, 423.
- Hegyí, D. J. & Olive, K. A., 1986. *Astrophys. J.*, **303**, 56.
- Kent, S. M., 1984. *Astrophys. J. Suppl. Ser.*, **56**, 105.
- Kent, S. M., 1986. *Astr. J.*, **91**, 1301.
- Monet, D. G., Richstone, D. O. & Schechter, P. L., 1981. *Astrophys. J.*, **245**, 454.
- Persic, M. & Salucci, P., 1985. *Soc. Ital. di Fisica*, **1**, 133.
- Persic, M. & Salucci, P., 1986. *Mon. Not. R. astr. Soc.*, **223**, 303 (Paper I).
- Peterson, C. J., 1980. *Astr. J.*, **85**, 226.
- Peterson, C. J., 1982. *Publs astr. Soc. Pacif.*, **94**, 409.
- Rohlf, K., 1982. *Astr. Astrophys.*, **105**, 296.
- Rubin, V. C., Ford, W. K. & Thonnard, N., 1980. *Astrophys. J.*, **238**, 471.
- Rubin, V. C., Ford, W. K., Thonnard, N. & Burstein, D., 1982. *Astrophys. J.*, **261**, 439.
- Rubin, V. C., Burstein, D., Ford, W. K. & Thonnard, N., 1985. *Astrophys. J.*, **289**, 81.
- Salucci, P., 1986. *PhD dissertation*, SISSA, Trieste.
- Sancisi, R., Allen, R. J. & Sullivan, W. T. III, 1979. *Astr. Astrophys.*, **78**, 217.
- Simien, F. & de Vaucouleurs, G., 1986. *Astrophys. J.*, **302**, 564.
- Tinsley, B. M., 1981. *Mon. Not. R. astr. Soc.*, **194**, 63.
- Tully, R. B. & Fisher, J. R., 1977. *Astr. Astrophys.*, **54**, 661.
- van Albada, T. S. & Sancisi, R., 1986. *Phil. Trans. R. Soc. Lond. A*, **320**, 447.
- van Albada, T. S., Bahcall, J. N., Begeman, K. & Sancisi, R., 1985. *Astrophys. J.*, **295**, 305.
- van der Kruit, K. C., 1987. *Astr. Astrophys.*, **173**, 49.
- van Moorsel, G. A., 1982. *Astr. Astrophys.*, **107**, 66.
- van Moorsel, G. A., 1983a. *Astr. Astrophys. Suppl. Ser.*, **53**, 271.
- van Moorsel, G. A., 1983b. *Astr. Astrophys. Suppl. Ser.*, **54**, 1.
- van Moorsel, G. A., 1983c. *Astr. Astrophys. Suppl. Ser.*, **54**, 19.
- Visvanathan, N. & Griersmith, D., 1979. *Astrophys. J.*, **230**, 1.
- Whitmore, B. C., 1984. *Astrophys. J.*, **278**, 71.
- Whitmore, C. W., McElroy, D. B. & Schweizer, F., 1987. *Astrophys. J.*, **314**, 439.